# A STOCHASTIC MODEL OF THE REPETITIVE ACTIVITY OF NEURONS

C. DANIEL GEISLER *and* JAY M. GOLDBERG

*From the Electrical Engineering Department and Laboratory of Neurophysiology, University of Wisconsin, Madison, and the Department of Physiology, University of Chicago, Chicago*

ABSTRACT A recurrent model of the repetitive firing of neurons responding to stimuli of long duration is given. The model assumes a deterministic threshold potential and a membrane potential which is composed of both deterministic and random components. The model accurately reproduces interval statistics obtained from different neurons discharging repetitively over a wide range of discharge rates. It is shown that the model has three important parameters; the time course of threshold recovery following a discharge, the variance of the random component, and the level of excitatory drive. The model is extended, by the use of hyperpolarizing afterpotentials, to include negative correlation between successive interspike intervals.

## INTRODUCTION

Even under controlled experimental conditions, the discharge characteristics of single neurons exhibit some degree of irregularity. Experiments sometimes have involved the presentation of identical, near-threshold stimuli to a nerve fiber (e.g. Verveen, 1961); the fiber, apparently on a random basis, discharges in response to some stimuli, but not to others. Other experiments have dealt with the intervals between successive discharges in a long train of impulses evoked either by natural or artificial stimuli (e.g. Buller, Nicholls, and Ström, 1953; Hagiwara, 1954; Kuffler, Fitzhugh, and Barlow, 1957; Viernstein and Grossman, 1961); the interspike intervals are never constant. Observations of this nature have led to the development of stochastic models of the discharge of the neuron (Landahl, 1941; Hagiwara, 1954; McGill, 1963; Perkel, Moore, and Segundo, 1963; Fetz and Gerstein, 1963; Gerstein and Mandelbrot, 1964). In this paper, we will examine a stochastic model of the type originally suggested by Landahl (1941) and Hagiwara (1954), demonstrate its ability to account for the interspike interval distributions generated during repetitive activity, and illustrate its behavior as its parameters are systematically varied.

The model to be explored is presented schematically in Fig. 1. Two waveforms are represented in the figure; the threshold and the membrane potentials. The membrane potential is composed of two independent components, a deterministic voltage $D_F$, and an additive random voltage $N(t)$ with a Gaussian amplitude distribution. Whenever the membrane potential exceeds the threshold voltage, the cell discharges. After the occurrence of an impulse, the threshold is infinite for a short time and then gradually returns to its resting value. It is assumed that the random

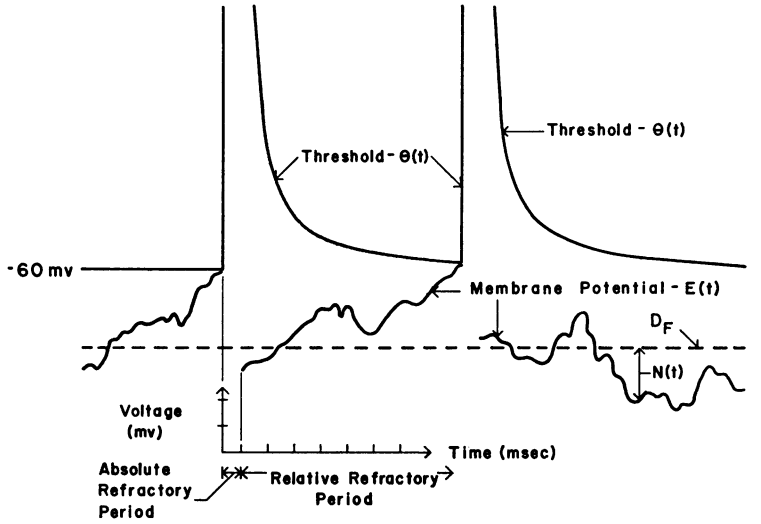


FIGURE 1 Diagram illustrating the characteristics of the recurrent event model used in this paper. The threshold function $\Theta(t)$ is given by equation 4 with $\tau = 5$ msec.

noise $N(t)$ following a discharge is uncorrelated with the random noise that preceded the occurrence of that discharge.

Studies of such models have employed several techniques. Ten Hoopen and Verveen (1963) and Fetz and Gerstein (1963) used electronic equipment to generate actual voltages corresponding to the threshold and membrane potentials. Other workers (Landahl, 1941; Hagiwara, 1954; Viernstein and Grossman, 1961; Siebert and Gray, 1963; Ten Hoopen, Den Hertog, and Reuver, 1963; Goldberg, Adrian, and Smith, 1964) attempted to compute the necessary interval distributions by means of mathematical equations. Unfortunately, the equations presented do not lead to correct expressions for the interval distributions generated using any well known Gaussian random process.[1]

[1]The models of Landahl (1941), Hagiwara (1954), Viernstein and Grossman (1961), and Goldberg, Adrian, and Smith (1964) are characterized by the property that, if there were no refractory period, the interval distributions would be exponential. However, it cannot be assumed that Gaussian noise generally produces such distributions, because a nonexponential distribution has been obtained using RC-filtered Gaussian noise (Rice, 1958, equation 113).

In the model described in the present paper, the necessary waveforms have been simulated on a digital computer, a procedure previously employed by Weiss (1964).

## DERIVATION OF THE MODEL

In the model, a discharge occurs whenever the membrane potential $E(t)$ exceeds the threshold potential $\Theta(t)$. The potentials cannot be represented as continuous waveforms by a digital computer. Each of the potentials was therefore represented by a sequence of numbers. The two sequences were compared term by term. Whenever the number representing the membrane potential equalled or exceeded the number representing the threshold potential, a discharge was considered to have occurred, and the process was begun again at $t = 0$.

The numbers representing the threshold potential $\Theta(t)$ were obtained by evaluating the threshold function at the desired instants of time. Because of the presence of a random component, the generation of numbers representing the membrane potential $E(t)$ was more complicated. The random component $N(t)$ was chosen to have a Gaussian amplitude distribution with a mean of zero. The first step was the generation of approximately normally distributed pseudorandom numbers $X_0, X_1, \ldots, X_n$. Each $X_i$ was calculated by adding together 16 uniformly distributed pseudorandom numbers. In order to arrive at a sequence of numbers representing the random component $N(t)$, the $X_i$'s must be appropriately combined; the actual combination depending upon the spectrum of $N(t)$. We chose as the spectrum

$$S(f) = \frac{f_1/\pi}{f^2 + f_1^2}, \tag{1}$$

the output spectrum of an RC low-pass filter whose input is white noise. The autocorrelation function corresponding to this spectrum is $\Phi(t) = \exp(-2\pi f_1|t|)$. Levin (1960) has shown that the set of numbers

$$\begin{aligned} N(0) &= X_0 \\ N(i\Delta t) &= [1 - \exp(-4\pi f_1 \Delta t)]^{1/2} X_i \\ &\quad + [\exp(-2\pi f_1 \Delta t)] N[(i-1)\Delta t], \qquad i = 1, \cdots, n, \end{aligned} \tag{2}$$

has the same stochastic properties as does the set of numbers obtained from sampling, at equal intervals of time $\Delta t$, a Gaussian noise with the spectrum of equation 1. It is easily verified that the numbers generated by equation 2 have an approximately Gaussian amplitude distribution, a mean of zero, and an autocorrelation function

$$\Phi(i\Delta t) = \exp(-2\pi f_1 i \Delta t), \qquad i = 0, 1, \cdots, n. \tag{3}$$

Addition of the numbers $N(0), N(\Delta t), \ldots, N(n\Delta t)$ to the deterministic component of the membrane potential gives a sequence of numbers representing the membrane potential $E(t)$.

Representing the continuous waveforms by sequences of numbers introduces

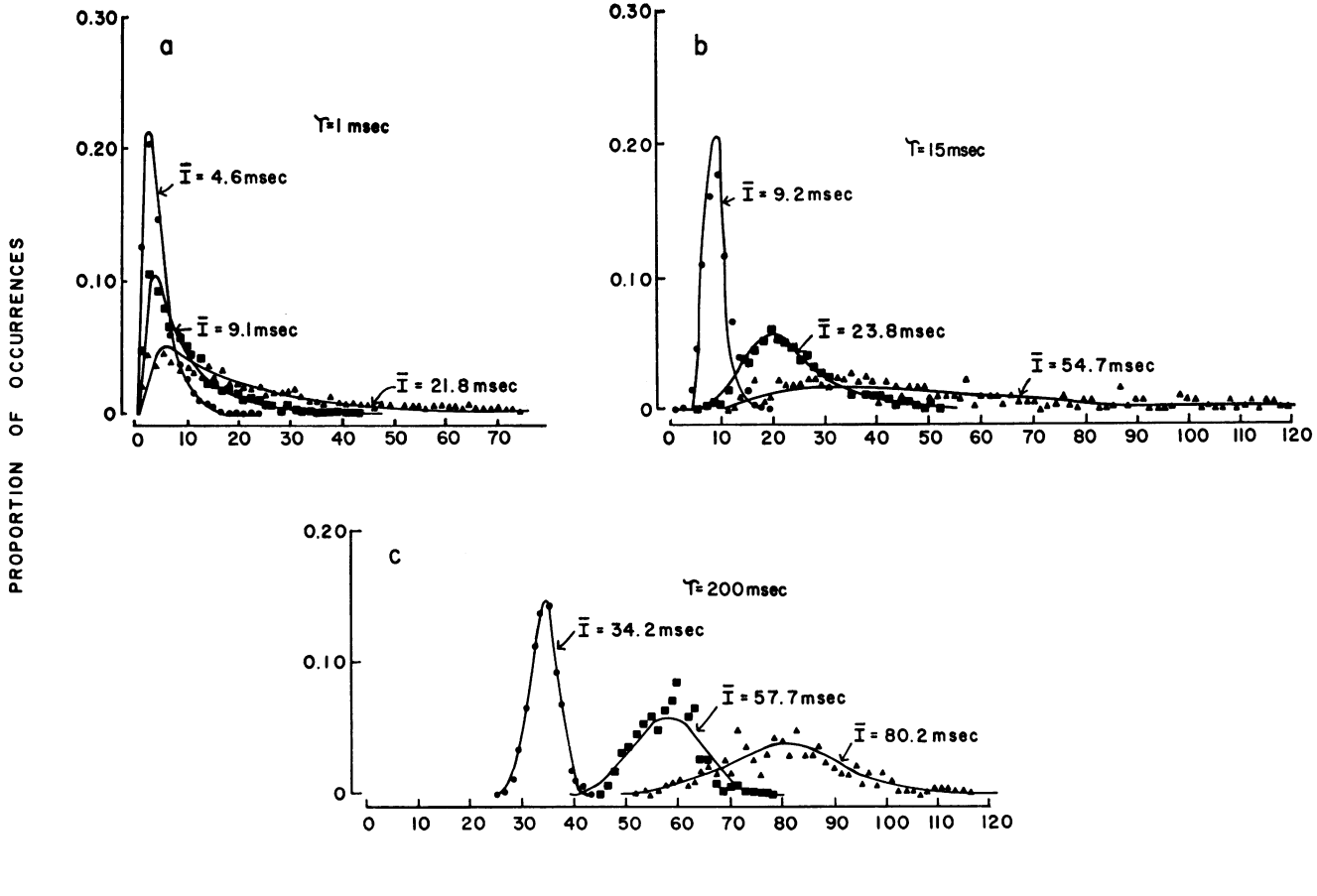
a
τ=1 msec
Ī = 4.6msec
Ī = 9.1msec
Ī = 21.8 msec
b
τ=15msec
Ī = 9.2msec
Ī = 23.8msec
Ī = 54.7msec
c
τ=200msec
Ī = 34.2msec
Ī = 57.7msec
Ī = 80.2 msec
PROPORTION OF OCCURRENCES
TIME (MSEC)

FIGURE 2

errors into our results. The magnitude of these errors is related to the magnitude of the sampling interval $\Delta t$. In most of our calculations, the value of $\Delta t$ was chosen to have a value of $0.05/f_1$, although smaller values were used occasionally. The effects of varying the value of $\Delta t$, and hence of varying the magnitude of the computational errors, will be described below (see Results).

Approximately 1000 intervals were generated to form each of the theoretical interval distributions and interval statistics presented in the paper. All calculations were performed on the Control Data Corporation 1604 computer of the University of Wisconsin Computing Center.

## RESULTS

*Applications of the Model.* Interspike interval distributions generated by the model closely resemble the interspike interval distributions derived from neurons of the superior olivary complex of the cat responding to acoustic stimuli of long duration. Fig. 2 shows experimental data from three different neurons plotted as normalized interspike interval histograms. Histograms generated by the model are also displayed and a close match is observed between the empirical and theoretical data. The ability of the model to simulate the behavior of individual superior olivary neurons is further illustrated in Fig. 3, which presents the relations between the mean interval and standard deviation of intervals for each of the three neurons of Fig. 2 and the corresponding relations generated by the model. The fit between the theoretical and empirical relations is excellent over a wide range of discharge rates.

The following parameters were used to generate the theoretical data of Figs. 2 and 3. In all of the calculations, $N(t)$, the random component of the membrane potential, had a standard deviation of 1 mv and half-power frequency of 500 cycle/sec. The threshold function $\Theta(t)$ (See Fig. 1) consisted of an absolute refractory period $R$ of 0.7 msec followed by a relative refractory period described by the function (Fuortes and Mantegazzini, 1962)

---

FIGURE 2 A comparison of distributions derived from neurons of the superior olivary complex with theoretical distributions. Each graph includes interspike interval distributions (points), with various values of mean interval $\bar{I}$, derived from a single neuron, together with corresponding distributions (smooth curves) generated by the model using a single value of threshold time constant $\tau$. In these graphs, the abscissa represents the value of the interval in msec; the ordinate, the proportion of intervals with values that fall within the limits of a 1 msec time bin. *a:* Theoretical distributions, $\tau = 1$ msec; neural distributions, unit 62-157-4. *b:* Theoretical distributions, $\tau = 15$ msec; neural distributions, unit 62-394-1. *c:* Theoretical distributions, $\tau = 200$ msec; neural distributions, unit 62-239-2. Each theoretical distribution is a smooth curve fitted by eye to an interspike interval histogram generated by the model; $\sigma_N = 1$ mv, $f_1 = 500$ cycle/sec, $\Delta t = 0.1$ msec. Neural data are from the study by Goldberg, Adrian, and Smith (1964).

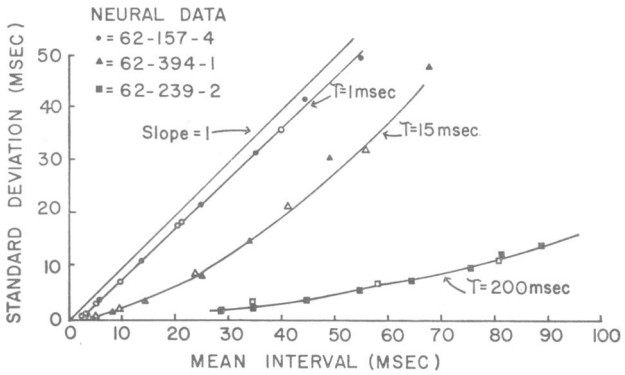


FIGURE 3 Mean interval and standard deviation of intervals obtained from the model and from superior olivary neurons. Each set of solid symbols depicts data derived from one individual neuron, and the corresponding set of open symbols depicts theoretical data for one value of $\tau$. Each smooth curve was fitted by eye to one set of theoretical data; $\sigma_N = 1$ mv, $f_1 = 500$ cycle/sec, $\Delta t = 0.1$ msec. Physiological data were obtained by dividing trains of impulses into groups of 20 consecutive intervals, determining the mean and standard deviation for each group, and then averaging the means and standard deviations for all groups possessing similar means. For further details, see Goldberg, Adrian, and Smith (1964).

$$\Theta(t) = -60 + \exp[-(t - R)/\tau]/\{1 - \exp[-(t - R)/\tau]\} \text{ mv},$$
$$t \geq R = 0.7 \text{ msec}. \quad (4)$$

Such a function starts at infinity at $t = 0.7$ msec and approaches $-60$ mv as $t$ approaches infinity. The threshold time constant $\tau$ was held fixed while modelling the activity of any one neuron. Once this time constant was set, only $D_F$, the deterministic component of the membrane potential, had to be varied to simulate the behavior of a single neuron under different conditions of excitatory drive. A different time constant $\tau$ was needed to simulate the activity of each of the three different neurons.

The activity of other types of neurons can be approximated by the model. Buller, Nicholls, and Ström (1953) and Hagiwara (1954) studied the relation between the mean interval and standard deviation of intervals in frog muscle spindle axons under conditions of steady stretch. Fig. 4 shows some of the data points obtained by the former workers as well as data generated by the model with $\tau = 81$ msec. The fit between the theoretical and experimental points, while not as good as that seen for superior olivary neurons, is satisfactory; the theoretical data also provide a reasonably close fit to the data of Hagiwara (1954). Fig. 4 also demonstrates that the data obtained by Biscoe and Taylor (1963) from chemoreceptor fibers of the carotid body of the cat are successfully matched by the model when the value of $\tau$ is set to 8.5 msec. Buller, Nicholls, and Ström (1953) and Biscoe and Taylor (1963) observed that, for long mean intervals, the slope of the relation between the mean

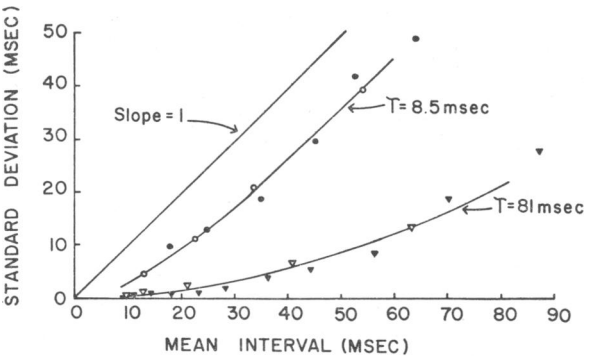


FIGURE 4 Mean interval and standard deviation of intervals derived from the model, from amphibian stretch receptors, and from chemoreceptors of the cat carotid body. Data from stretch receptors (▼) are from Table 1 of Buller, Nicholls, and Ström (1953); corresponding theoretical data (▽), $\tau = 81$ msec. Data from carotid body chemoreceptors (●) are median values taken from Fig. 2 (perfused) of Biscoe and Taylor (1963); theoretical data (○), $\tau = 8.5$ msec. Each smooth curve was fitted by eye to one set of theoretical data; $\sigma_N = 1$ mv, $f_1 = 500$ cycle/sec, $\Delta t = 0.1$ msec.

interval and standard deviation of intervals approached a slope of unity. Similar behavior is exhibited by the data generated by the model (see Discussion).

Katz (1950) has found that, in the amphibian muscle spindle, there is a linear relation between the local depolarization produced by steady stretch and the frequency of impulses for rates up to 300 impulses/sec. Linear relations between the magnitude of the generator potential and the frequency of discharge have also been observed over wide ranges of excitation in other sensory neurons (MacNichol, 1956; Fuortes, 1958; Lippold, Nicholls, and Redfearn, 1960; Loewenstein, 1960; Wolbarsht, 1960; Terzuolo and Washizu, 1962). Fig. 5 presents the theoretical relations between the average frequency of discharge and the mean membrane potential $D_F$ for several values of $\tau$. Note that the relation obtained with the time constant appropriate for the muscle spindle ($\tau = 81$ msec) is almost linear. The other curves in Fig. 5 are also approximately linear throughout a large part of their range. Therefore, the relations between depolarization and discharge rate obtained with the model are similar to the empirical relations observed in a number of neurons. It should be noted that curves similar to those of Fig. 5 can be generated by an essentially deterministic model (Harmon, 1961).

*The Effect of Varying the Parameters of the Random Component.* The parameters of the random component $N(t)$ are the half-power frequency $f_1$, the standard deviation $\sigma_N$, and the sampling interval $\Delta t$. In the above calculations all of these parameters were held constant. The effects of varying these parameters will be described in this section.

*Half-power frequency:* The effects of variation of the half-power frequency $f_1$ of the low-pass noise are readily visualized; the probability of discharge

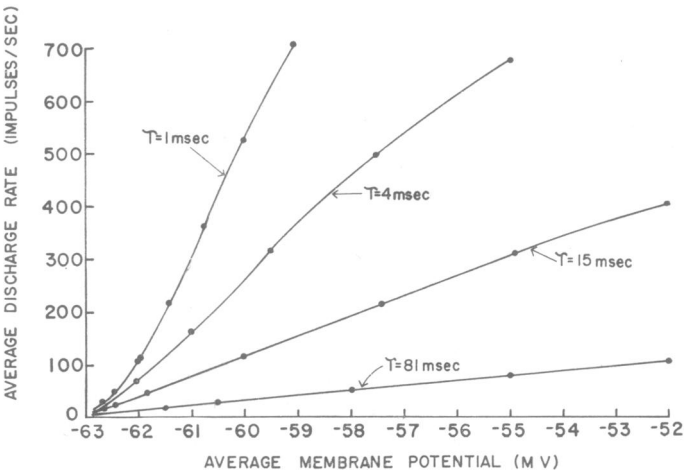


FIGURE 5 Average rate of discharge vs. average membrane potential. Each point summarizes data generated by the model with the indicated value of $\tau$; $f_1 = 500$ cycle/sec, $\sigma_N = 1$ mv, $\Delta t = 0.1$ msec. Smooth curves were fitted by eye.

within a fixed time period decreases as $f_1$ decreases. It should be possible, however, to compensate partly for a decrease in $f_1$ by an increase in the mean excitatory input. That changes in $f_1$ do not alter the basic properties of the model is illustrated in Fig. 6, where the relations between the mean interval and the standard deviation of intervals for various values of the time constant $\tau$ and of $f_1$ are presented. With the time constant held fixed, a decrease in the half-power frequency has the effect of slightly shifting the relation to the left. However, the variations among the curves

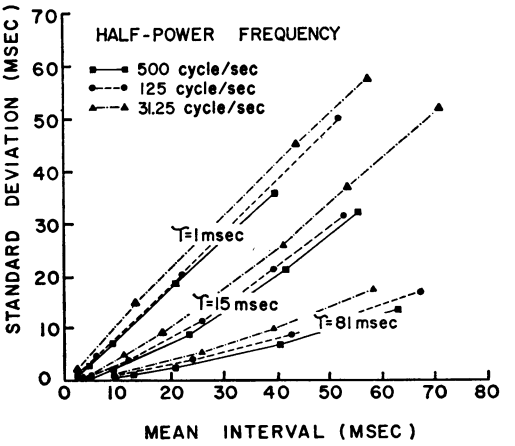


FIGURE 6 Mean interval vs. standard deviation of intervals. Each point summarizes data generated by the model using the indicated value of threshold time constant $\tau$ and of half-power frequency $f_1$; $\sigma_N = 1$ mv, $0.0031/f_1 \leq \Delta t \leq 0.05/f_1$.

for any one value of $\tau$ are small, and the curves could be brought into even better agreement by small changes in the value of $\tau$.

*Standard deviation:* The standard deviation $\sigma_N$ of the random component is a crucial parameter of the model. The relations between the mean interval and the standard deviation of intervals presented in Fig. 7 were obtained by holding the time constant $\tau$ at a value of 15 msec and systematically varying the value of $\sigma_N$. An increase in $\sigma_N$ results in a displacement of the relation to the left. This effect is

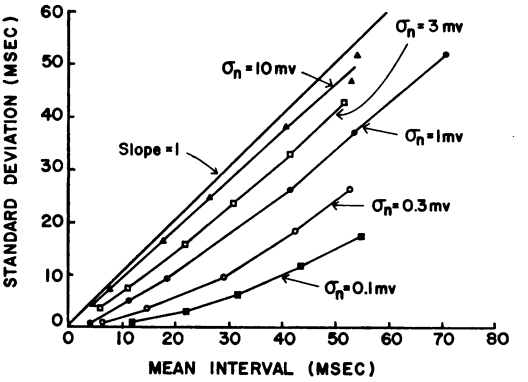


FIGURE 7 Mean interval vs. standard deviation of intervals. Each point was obtained from data generated by the model with the indicated value of noise standard deviation $\sigma_N$; $\tau = 15$ msec, $f_1 = 31.25$ cycle/sec, $0.1 \leq \Delta t \leq 1.6$ msec.

similar to that obtained when the value of $\tau$ is decreased. A comparison of Figs. 6 and 7 reveals that a hundredfold variation of $\sigma_N$, $\tau$ being fixed, is roughly equivalent to a seventyfold variation of $\tau$, $\sigma_N$ being held constant.

In the model, it is assumed that the variance of the random noise *N(t)* is time-invariant and also that it is independent of the average membrane potential. If the noise were due to thermal activity, for example, such assumptions would not be unreasonable. If, on the other hand, an important component of the fluctuation of membrane potential were due to the discrete nature of synaptic potentials, the assumptions would be oversimplifications. Stein (1965) has shown that, in situations where *N(t)* is wholly determined by randomly occurring synaptic potentials of the same exponential waveform, both the mean value and variance of the membrane potential are functions of time and of the rate of occurrence of the synaptic potentials. Only if the rate of occurrence of the synaptic potentials becomes large, and if the time constant characterizing the synaptic potentials becomes small compared with the other time constants of the system does the random process described by Stein (1965) approach the process utilized in our calculations; namely, a time-invariant Gaussian process whose spectrum is given by equation 1.

*Sampling interval:* Most of our data were generated with the value of

the sampling interval $\Delta t$ set to $0.05/f_1$. Smaller values of $\Delta t$, some as low as $0.0031/f_1$, were sometimes used to achieve better resolution. That errors result from representing the membrane potential as a sequence of numbers is indicated by the fact that data obtained when $\Delta t = 0.05/f_1$ differed from data obtained when $\Delta t$ was set to $0.0031/f_1$, all other parameters of the model being held constant. However, the differences observed when the value of $\Delta t$ was decreased were almost completely compensated for by a decrease in $D_F$, the mean value of the membrane potential. Stated in other terms, variations in $\Delta t$ affected the relation between the average rate of discharge and $D_F$, but did not alter the shapes of the interval distributions obtained with the model or the relations between the mean interval and standard deviation of intervals.

It can be shown that our method of determining a threshold crossing is equivalent to passing the membrane potential $E(t)$ through a sample and zero order hold circuit and determining when the resulting staircase approximation of $E(t)$ crosses the threshold potential $\Theta(t)$. Ragazinni and Franklin (1958) have shown that the staircase approximation approaches the unsampled waveform $E(t)$ as $\Delta t$ approaches zero. A small amount of data was obtained from the model with $\Delta t$ set to $0.00031/f_1$. The fact that these data differed little from data generated with $\Delta t = 0.0031/f_1$ suggests that the staircase approximations corresponding to these smaller values of $\Delta t$ are closely convergent to the unsampled waveform $E(t)$.

*Extension of the Model to Account for the Correlation between Neighboring Intervals.* In the model presented above, the generation of impulses is a recurrent event, which implies that the interspike intervals occurring during repetitive discharge are statistically independent of one another. For some neurons, the intervals are indeed statistically independent, at least in a linear sense (Buller, Nicholls, and Ström, 1953; Hagiwara, 1954; Rodieck, Kiang, and Gerstein, 1962; Goldberg, Adrian, and Smith, 1964). Other neurons, however, exhibit a negative correlation between the values of adjacent intervals in a record (Hagiwara, 1949; Kuffler, Fitzhugh, and Barlow, 1957; Viernstein and Grossman, 1961; Goldberg, Adrian, and Smith, 1964). One explanation of this negative correlation is that it is due to the summation of hyperpolarizing afterpotentials which follow each discharge (Goldberg, Adrian, and Smith, 1964), a mechanism suggested in another context by Eccles (1953). That this mechanism will result in negative correlation of the sort observed empirically can be demonstrated by means of an extension of our basic model.

The extended model is illustrated in Fig. 8. The threshold function is that of equation 4. The membrane potential $E(t)$ is the sum of two components, $N(t)$, a random waveform generated by the same process as that used in the recurrent model, and $D(t)$, a function which describes the reestablishment of the transmembrane depolarization following each impulse. The time course of $D(t)$ is determined by a hyperpolarizing afterpotential $P(t)$ such that

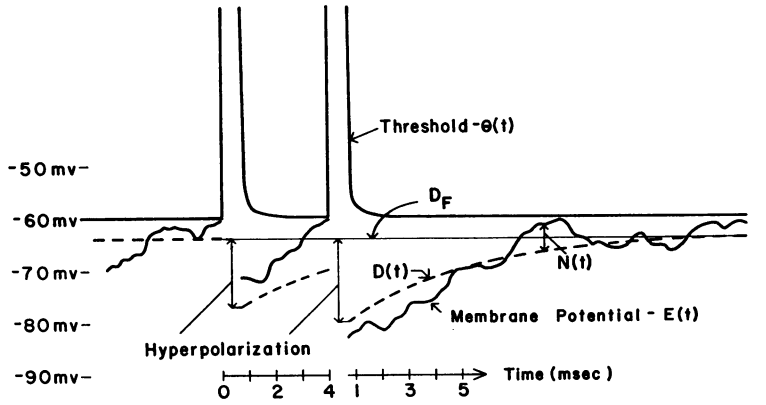


FIGURE 8 Diagram illustrating the characteristics of the extended model. The threshold function $\theta(t)$ is given by equation 4 with $\tau = 1$ msec. The decay of the hyperpolarization is exponential with a time constant of approximately 4.3 msec.

$$D(t) = D_F + P(t)$$
$$= D_F + (D_I - D_F) \exp[-(t - R)/\phi], \qquad t \geq R = 0.7 \text{ msec}, \qquad (5)$$

where $D_I$ is the value of the membrane potential at the beginning of the afterpotential, $D_F$ the value of the membrane potential in the fully recovered state, and $\phi$ the time constant of decay of the afterpotential. $D_F$ is dependent only upon the level of excitatory input. $D_I$ is not constant, but varies depending upon past history. On the basis of data from spinal motoneurons of the cat (Coombs, Eccles, and Fatt, 1955), $D_I$ is set to one half the difference between $-90$ mv and the value of $D(t)$ at the instant that the preceding discharge occurred. For example, if a discharge occurs when $D(t)$ is $-64$ mv (the value of $D_F$ in Fig. 8), $D_I$ for the succeeding afterpotential is set to $-77$ mv. If a discharge occurs when $D(t)$ is $-70$ mv (see the second impulse of Fig. 8), $D_I$ is set to $-80$ mv. A short interval will cause $D_I$ to have a relatively large magnitude, and, consequently, the next interval will tend to be a long one. Negative correlation between the values of adjacent intervals will result since there will be a tendency for short intervals to be followed by long ones and vice versa.

Data generated by the extended model are presented in Fig. 9. The relations between the mean interval and the standard deviation of intervals for three values of $\sigma_N$ are shown in Fig 9*a*. For each of the curves, the time constants of the threshold and the afterpotential were fixed at 0 and 9 msec, respectively. As has been seen in Fig. 7, increasing the value of $\sigma_N$ shifts the relations to the left. Note that the interval statistics behave very much like those generated by the recurrent model, even though the intervals are now no longer independent of one another. In fact, the data of Unit 62-394-1 (see Fig. 3) fall close to the relation shown in Fig. 9*a*

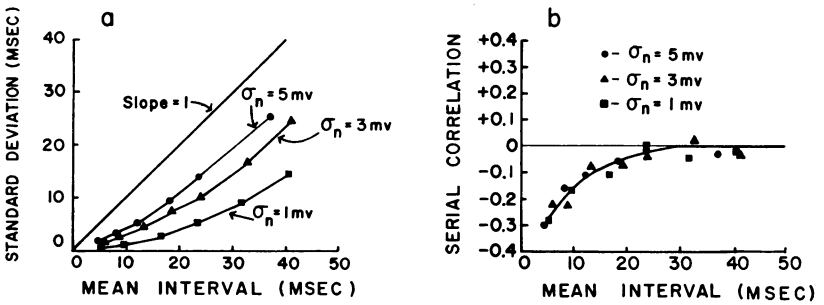


FIGURE 9 Data derived from the extended model, with threshold time constant $\tau$ held fixed at zero msec and the afterpotential time constant $\phi$ held fixed at 9 msec. *a:* mean interval vs. standard deviation of intervals. Each point is based on data obtained from approximately 1000 consecutive intervals generated with the indicated value of noise standard deviation $\sigma_N$; $f_1 = 31.25$ cycle/sec, $0.1 \leq \Delta t \leq 1.6$ msec. *b:* correlation analysis. Each point in *b* is based on the same sample of intervals that was used in the generation of the data point in *a* having the same mean interval. The smooth curve was fitted by eye.

for $\sigma_N = 3$ mv and could be very well approximated if $\sigma_N$ were set slightly below 3 mv.

The serial correlation coefficients $r_k$ were computed by pairing the $i$th and the $(i + k)$th intervals. Fig. 9*b* shows the relations between the mean interval and $r_1$ for the data summarized in Fig. 9*a*. The relations for the different values of $\sigma_N$ are indistinguishable. The correlation coefficients decrease in magnitude as mean interval increases and become negligible for mean intervals greater than approximately 30 msec. The lack of correlation when the mean interval is greater than 30 msec is to be expected, because, for intervals of this value, the afterpotential has decayed to less than 5% of its initial value. Hence, the effect of the past interval is largely erased. The increase of correlation with decreasing mean interval is caused by the fact that more and more intervals occur with significant memory contained in the afterpotential. None of the coefficients $r_k$, $k = 2$ to 5, differed significantly from zero. There is remarkably good agreement between the data presented in Fig. 9*b* and that obtained from certain neurons of the superior olivary complex (Goldberg, Adrian, and Smith, 1964) and cochlear nucleus (Goldberg and Greenwood, 1966).

## DISCUSSION

*Simulation of the Interval Distributions of a Single Neuron.* In either the recurrent or extended models, the timing of discharges during repetitive activity is jointly determined by the asymptotic excitatory drive [i.e. $\Theta(\infty) - D_F$], the time course of recovery from preceding activity, and a random component responsible for the fluctuations of interspike intervals. One of the basic assumptions of the model is that the time constants describing the recovery processes of any given

neuron are constant under all conditions of excitatory drive. We will, therefore, in discussing the variations in the interval distributions derived from the model of an individual neuron, confine our attention to the effects of variations of the asymptotic excitatory drive and of the parameters of the random component.

An attractive feature of the models is the relatively simple manner by which the variations in the interval distributions derived from an individual neuron can be simulated. Variations in the asymptotic excitatory drive of the model, all other parameters being held constant, have accounted for the variations in the interval statistics of auditory neurons as the frequency and intensity of tonal stimuli are varied (Figs. 2, 3, and 9*b*) and for the variations in the interval statistics of the amphibian stretch receptor and the chemoreceptor of the cat carotid body (Fig. 4). If, indeed, the interval distributions derived from a single neuron responding in a sustained manner to steady stimulation are determined by the asymptotic excitatory drive, then other statistical parameters describing the discharge of the neuron should be a function of the asymptotic excitatory drive and, hence, of the mean rate of discharge. This proposition is supported by a number of observations. For amphibian stretch receptors (Buller, Nicholls, and Ström, 1953; Hagiwara, 1954), for the chemoreceptors of the carotid body (Biscoe and Taylor, 1963), and for neurons of the ventrobasal complex (Werner and Mountcastle, 1963), the superior olivary complex (Goldberg, Adrian, and Smith, 1964), and the cochlear nucleus (Goldberg and Greenwood, 1966), the standard deviation of intervals is systematically related to the mean interval. Moreover, for those auditory neurons whose discharge is characterized by negative correlation between adjacent intervals in a record, there is a systematic relation between the mean interval and the degree of correlation (Goldberg, Adrian, and Smith, 1964; Goldberg and Greenwood, 1966). A severe test of the proposition may be made by comparing the characteristics of sustained discharge of a given neuron in response to different stimuli which result in the same mean discharge rate. It was found, when such studies were carried out in the superior olivary complex (Goldberg, Adrian, and Smith, 1964) and in the cochlear nucleus (Goldberg and Greenwood, 1966), that both the standard deviation of intervals and the correlation between neighboring intervals were essentially similar for all tonal stimuli which led to the same mean discharge rate, even when it could be reasonably inferred that the various stimuli that were employed activated different combinations of excitatory and inhibitory pathways.

The effects of variations of the parameters of the random component on the behavior of the models is illustrated in Figs. 6, 7, and 9. The half-power frequency of the spectrum of the random process does not play a major role in determining the relations between interval statistics. In contrast, the variance of the random component, while not affecting the correlation between neighboring intervals, has an important influence on the relation between the mean interval and standard deviation of intervals. The theoretical effects of increasing the variance of the random

component parallel the results of a study in which a comparison was made of the interval distributions derived from neurons of the cochlear nucleus responding to pure tones and to narrow bands of noise (Goldberg and Greenwood, 1966). Because one of the most conspicuous features of a narrow band noise is the variations in the envelope of the signal, the random fluctuations in excitatory drive should be greater when bands of noise, rather than tones, are employed as stimuli. Consistent with theoretical expectations, the use of bands of noise in place of tones affected the relation between the mean interval and the standard deviation of intervals, without influencing the relation between the mean interval and the degree of negative correlation between neighboring intervals.

*Simulation of the Interval Statistics Derived from Different Neurons.* The interval distributions generated by the recurrent model are determined by the values of the half-power frequency $f_1$ of the random component, and the ratio $[\Theta(t) - D_F]/\sigma_N$, where $\Theta(t)$ is the threshold function, $D_F$ the mean membrane potential, and $\sigma_N$ the standard deviation of the random component. Variations of $f_1$ do not affect the shapes of the interval distributions to any great extent. In contrast, the ratio $[\Theta(t) - D_F]/\sigma_N$ is of importance in determining the distributions generated by the model. More particularly, the ratio $\Theta(t)/\sigma_N$ determines the shapes of the interspike interval distributions and the relation between the mean interval and the standard deviation of intervals, whereas the ratio $D_F/\sigma_N$ determines the mean rate of discharge, once the values of $\Theta(t)/\sigma_N$ and $f_1$ are specified. A similar conclusion was reached by Verveen and Derksen (1965).

The differences in the interspike interval distributions obtained from different neurons can be accounted for if it is assumed that the ratio $\Theta(t)/\sigma_N$ is fixed for each neuron but may vary from one neuron to another. The value of the ratio and, hence, the shapes of the interval distributions and the relation between the mean interval and standard deviation of intervals are affected by variations of either $\Theta(t)$ (Figs. 2 and 3) or $\sigma_N$ (Fig. 7). One cannot, from an inspection of the interval distributions derived from a given neuron, determine the absolute value of $\Theta(t)$ unless $\sigma_N$ is specified and vice versa. Goldberg, Adrian, and Smith (1964) assumed that $\sigma_N$ was the same for all neurons. Hence, they concluded that the differences in interval distributions derived from different neurons could be explained most easily by assuming that neurons differed from one another in the time required to recover from the effects of a discharge. Our lack of knowledge of possible variations of $\sigma_N$ among neurons makes such a conclusion premature.

Neurons differ from one another not only in the shapes of their interspike interval distributions but also in the degree of negative correlation displayed between the values of adjacent intervals in a record. In a study of neurons of the cochlear nucleus (Goldberg and Greenwood, 1966), for example, it was found that, despite the fact that two neurons generated similar interval histograms, adjacent intervals of one of the neurons might display a relatively high degree of negative

correlation, whereas those of the other neuron might not. These latter differences may be explained by reference to the properties of the extended model. In this model, the timing of discharges is influenced by two recovery processes, an afterpotential $P(t)$ which results in the summation of the effects of successive impulses and a threshold potential $\Theta(t)$ which does not result in such summation. In the extended model, the shapes of the interval distributions are determined by the ratio $[\Theta(t) - P(t)]/\sigma_N$ and the degree of negative correlation is determined by the relative values of $\phi$ and $\tau$, the time constants of the afterpotential and the threshold functions, respectively. If $\phi \gg \tau$, then the timing of discharges will be primarily under the influence of the afterpotential and the neuron will display a relatively high degree of negative correlation, at least at high rates of discharge. If, on the other hand, $\tau \gg \phi$, then the extended model approaches the recurrent model in its properties and there will be no correlation.

*The General Characteristics of the Models.* All of the interval distributions generated by the models appear to be unimodal and to approach exponential distributions for sufficiently large values of time $t$. In order to define the general characteristics of the distributions, it is convenient to plot them in semilogarithmic coordinates.[2] Almost all of the distributions, when so plotted, define curves whose slopes, for values of $t$ greater than the mode, continually decrease and asymptotically approach constant values. Interval distributions with these characteristics have been obtained from a number of peripheral nerve fibers, including the amphibian stretch receptor (Buller, Nicholls, and Ström, 1953; Hagiwara, 1954), the limulus optic nerve (McGill, 1963), the chemoreceptor of the carotid body (Biscoe and Taylor, 1963), and auditory nerve fibers (Weiss, 1964), as well as from such central neurons as spinal interneurons (Hunt and Kuno, 1959), retinal ganglion cells (Kuffler, Fitzhugh, and Barlow, 1957; Levick, Bishop, Williams, and Lampard, 1961), and neurons of the lateral geniculate body (Levick, Bishop, Williams, and Lampard, 1961), the cochlear nucleus (Grossman and Viernstein, 1961; Rodieck, Kiang, and Gerstein, 1962; Pfeiffer and Kiang, 1965; Goldberg and Greenwood, 1966), the motor cortex (Martin and Branch, 1958), the midbrain reticular formation (Amassian, Macy, and Waller, 1961), the ventrobasal complex (Poggio and Viernstein, 1964), and the superior olivary complex (Goldberg, Adrian, and Smith, 1964). Other neurons (Martin and Branch, 1958; Hunt and Kuno, 1959; Levick, Bishop, Williams, and Lampard, 1961; Viernstein and Grossman, 1961; Rodieck, Kiang, and Gerstein, 1962; Bishop, Levick, and Williams, 1964; Poggio and Viernstein, 1964; Smith and Smith, 1965; Pfeiffer and Kiang, 1965) generate distributions that cannot be accounted for by the models described in this paper. Many of these latter cases, however, might be represented by our models if some-

[2] The abscissa represents the value of the interval, and the ordinate represents the logarithm of the proportion of intervals with stated value.

what more complicated functions were employed to describe the recovery processes (Viernstein and Grossman, 1961), if the random waveforms were not restarted after each discharge (Weiss, 1964), and/or if the excitatory drive on the cell were randomly gated on and off (Smith and Smith, 1965).

Another property of the models is that approximately exponential distributions are obtained whenever $\Theta(\infty)$, the asymptotic value of threshold, is several units of $\sigma_N$ greater than $D_F$, the asymptotic value of the membrane potential (e.g. Fig. 2*a*, $\bar{I} = 21.8$ msec). Moreover, the relations between the mean interval $\bar{I}$ and the standard deviation of intervals $S$ of distributions obtained under such conditions are well described by the equation,

$$S = \bar{I} - K, \tag{6}$$

$K$ being a constant determined by the time constants of the model. In every case, the value of $K$ can be identified with the time required for the ratio $[\Theta(t) - P(t)]/\sigma_N$ to approach its asymptotic value (e.g. Fig. 3, $\tau = 1$ msec). Neurons displaying these characteristics have been reported by several workers (Buller, Nicholls, and Ström, 1953; Biscoe and Taylor, 1963; Goldberg, Adrian, and Smith, 1964; Goldberg and Greenwood, 1966). It is interesting to note that the exponential distributions and the relationship described by equation 6 are characteristic of data generated by a Poisson process with a dead time $K$.

We wish to thank C. E. Molnar for pointing out to us limitations in existing mathematical models of neural discharges and H. J. Wertz for helpful discussions on sampled waveforms.

This work was supported in part by the National Institutes of Health (Grants NB-00896, NB-05237, General Research Grant 1-501-FR-05435, and Special Fellowship Grant 5 F11 NB 1427-02 NSRA), and in part by the Research Committee of the University of Wisconsin Graduate School from funds supplied by the Wisconsin Alumni Research Foundation. The National Science Foundation, through the University of Wisconsin Computing Center, provided the 1604 computer used in this study.

*Received for publication July 14, 1965.*

## REFERENCES

AMASSIAN, V. E., MACY, J., JR., and WALLER, H. J., 1961, *Ann. New York Acad. Sc.*, **89**, 883.

BISCOE, T. J., and TAYLOR, A., 1963, *J. Physiol.*, **168**, 332.

BISHOP, P. O., LEVICK, W. R., and WILLIAMS, W. O., 1964, *J. Physiol.*, **170**, 598.

BULLER, A. J., NICHOLLS, J. G., and STRÖM, G., 1953, *J. Physiol.*, **122**, 409.

COOMBS, J. S., ECCLES, J. C., and FATT, P., 1955, *J. Physiol.*, **130**, 291.

ECCLES, J. C., 1953, The Neurophysiological Basis of Mind, London, Oxford University Press, 176.

FETZ, E. E., and GERSTEIN, G. L., 1963, *in* Quarterly Progress Report No. 71, Cambridge, Massachusetts, Research Laboratory of Electronics, Massachusetts Institute of Technology, 249.

FUORTES, M. G. F., 1958, *Am. J. Ophth.*, **46**, 210.

FUORTES, M. G. F., and MANTEGAZZINI, F., 1962, *J. Gen. Physiol.*, **45**, 1163.

GERSTEIN, G. L., and MANDELBROT, B., 1964, *Biophysic. J.*, **4**, 41.

GOLDBERG, J. M., ADRIAN, H. O., and SMITH, F. D., 1964, *J. Neurophysiol.*, **27**, 706.

GOLDBERG, J. M., and GREENWOOD, D. D., 1966, *J. Neurophysiol.*, in press.
GROSSMAN, R. G., and VIERNSTEIN, L. J., 1961, *Science,* **134,** 99.
HAGIWARA, S., 1949, *Bull. Physiog. Sc. Research Inst. Tokyo Univ.,* **3,** 19, (cited in Kuffler, Fitzhugh, and Barlow, 1957).
HAGIWARA, S., 1954, *Jap. J. Physiol.,* **4,** 234.
HARMON, L. D., 1961, *Kybernetik,* **1,** 89.
HUNT, C. C., and KUNO, M., 1959, *J. Physiol.,* **147,** 364.
KATZ, B., 1950, *J. Physiol.,* **111,** 261.
KUFFLER, S. W., FITZHUGH, R., and BARLOW, H. B., 1957, *J. Gen. Physiol.,* **40,** 683.
LANDAHL, H. D., 1941, *Bull. Math. Biophysics,* **3,** 141.
LEVICK, W. R., BISHOP, P. O., WILLIAMS, W. O., and LAMPARD, D. G., 1961, *Nature,* **192,** 629.
LEVIN, M. J., 1960, *Inst. Radio Engrs. Trans. Inform. Theory,* **6,** 545.
LIPPOLD, O. C. J., NICHOLLS, J. G., and REDFEARN, J. W. T., 1960, *J. Physiol.,* **153,** 209.
LOEWENSTEIN, W. R., 1960, *Nature,* **188,** 1034.
MACNICHOL, E. F., JR., 1956, *in* Molecular Structure and Functional Activity of Nerve Cells, (R. G. Grenell and L. J. Mullins, editors), Washington, American Institute of Biological Sciences, 34.
MARTIN, A. R., and BRANCH, C. L., 1958, *J. Neurophysiol.,* **21,** 368.
MCGILL, W. J., 1963, *in* Handbook of Mathematical Psychology, (R. D. Luce, R. R. Bush, and E. Galanter, editors), New York, John Wiley and Sons, Inc., **1,** 309.
PERKEL, D. H., MOORE, G. P., and SEGUNDO, J. P., 1963, *in* Biomedical Sciences Instrumentation, (F. Alt, editor), New York, Plenum Press, **1,** 347.
PFEIFFER, R. R., and KIANG, N. Y.-S., 1965, *Biophysic. J.,* **5,** 301.
POGGIO, G. F., and VIERNSTEIN, L. J., 1964, *J. Neurophysiol.,* **27,** 517.
RAGAZINNI, J. R., and FRANKLIN, G. F., 1958, Sampled-data Control Systems, New York, McGraw-Hill Book Co., Inc., 250.
RICE, S. O., 1958, *Bell Syst. Techn. J.,* **37,** 581.
RODIECK, R. W., KIANG, N. Y.-S., and GERSTEIN, G. L., 1962, *Biophysic. J.,* **2,** 351.
SIEBERT, W. M., and GRAY, P. R., 1963, *in* Quarterly Progress Report No. 71, Cambridge, Massachusetts, Research Laboratory of Electronics, Massachusetts Institute of Technology, 241.
SMITH, D. R., and SMITH, G. K., 1965, *Biophysic. J.,* **5,** 47.
STEIN, R. B., 1965, *Biophysic. J.,* **5,** 173.
TEN HOOPEN, M., DEN HERTOG, A., and REUVER, H. A., 1963, *Kybernetik,* **2,** 1.
TEN HOOPEN, M., and VERVEEN, A. A., 1963, *in* Nerve, Brain and Memory Models, (N. Weiner and J. P. Schade, editors), Amsterdam, Elsevier Publishing Co., 8.
TERZUOLO, C. A., and WASHIZU, Y., 1962, *J. Neurophysiol.,* **25,** 56.
VERVEEN, A. A., 1961, Fluctuation in excitability, Ph.D. thesis, University of Amsterdam.
VERVEEN, A. A., and DERKSEN, H. E., 1965, *Kybernetik,* **2,** 152.
VIERNSTEIN, L. J., and GROSSMAN, R. G., 1961, *in* Information Theory, Fourth London Symposium, (C. Cherry, editor), London, Butterworth and Co. (Publishers) Limited, 252.
WEISS, T. F., 1964, Technical Report No. 418, Cambridge, Massachusetts, Research Laboratory of Electronics, Massachusetts Institute of Technology.
WERNER, G., and MOUNTCASTLE, V. B., 1963, *J. Neurophysiol.,* **26,** 958.
WOLBARSHT, M. L., 1960, *J. Gen. Physiol.,* **44,** 105.